JTTEE5 17:316–322
DOI: 10.1007/s11666-008-9182-4
1059-9630/$19.00 © ASM International

Effect of Ball Milling of Feedstock Powder on Microstructure and Properties of TiN Particle-Reinforced Al Alloy-Based Composites Fabricated by Cold Spraying

W.-Y. Li, G. Zhang, C. Zhang, O. Elkedim, H. Liao, and C. Coddet

(Submitted October 11, 2007; in revised form January 22, 2008)

Dense Al5356/TiN composites with TiN particles uniformly dispersed in the matrix were produced by cold spraying (CS) using both the mechanically mixed (MM) and ball-milled (BM) powder blends with 50 wt.% TiN compared to that of CS pure Al5356 deposit. The microhardness of the composite deposited with the BM blend was three times higher than that of pure Al5356 coating. Compared to the coating deposited with the MM powder (MM composite), the hardness of the coating deposited with the BM powder (BM composite) was significantly increased owing to the increase of TiN volume fraction, which is comparable to that of the MM composite deposited with the 75 wt.% TiN feedstock. The adhesive strength of the composites was remarkably improved in comparison with the pure Al5356 coating because of the pinning effect of TiN particles. The coefficient of frication (COF) and wear rate (WR) were measured using a ball-on-disc tribometer. It was found that the COFs and WRs of the composites were much lower than those of pure Al5356 coating. Especially, the WRs of the MM and BM composites were, respectively, decreased by about 14 and 50 times than that of pure Al5356 deposit. This phenomenon could be ascribed that TiN particles contribute to a third-body abrasion in the following sliding process, which benefits the decrease of COF by rolling action partially instead of sliding action. For the BM composite, more and finer TiN particles present in the worn surface compared to the MM composite, which will be helpful to the further decrease of the COF and WR.

Keywords aluminum alloy, ball milling, cold spraying, dry sliding wear, metal matrix composites

1. Introduction

Aluminum and its alloys find applications in automobile, defense, and aerospace sectors in terms of their specific weight and thermal conductivity. However, they have poor tribological characteristics (Ref 1). The fabrication of Al and its alloys-based metal matrix composites (AMMCs) is of great significance in applications owing to their excellent combination of higher specific strength and improved wear resistance over their base alloys (Ref 1, 2). The particle-reinforced MMCs are among the most widely used composite materials, which can be produced through a number of routes including melt processing and powder metallurgy, such as casting, sintering, hot pressing (Ref 1-8), and thermal spraying (TS) (Ref 9).

Recently, the emerging cold spraying (CS) technique has been widely investigated owing to its high deposition efficiency and volume production of deposits or parts, including metals and alloys (Ref 10-13), composites (Ref 14-22), and even nanostructure materials (Ref 23, 24). In this process, the deposition of particles takes place through their intensive plastic deformation upon impact in a solid state at a temperature well below the melting point of spray material. Consequently, the deleterious effects such as oxidation, decomposition, and grain growth inherent to conventional TS techniques can be minimized or eliminated (Ref 10). The previous studies (Ref 14-19) showed that AMMCs could be produced by CS of a simple powder blend. However, the deposited MMCs had much less volume fraction of hard particles than that in the blend.

As noticed in the fabrication of MMCs by conventional routes (Ref 1-8), hard particle size and volume fraction, interface conditions will influence the mechanical properties and wear performance of MMCs. Although SiC has been studied extensively (Ref 1-7), the promising use of SiC particles as reinforces is restricted due to the possible reaction of Al with SiC to form Al_4C_3, which has poor mechanical properties and severe corrosion problem (Ref 2, 8). Therefore, the use of other ceramics that do not

W.-Y. Li, Shaanxi Key Laboratory of Friction Welding Technologies, School of Materials Science and Engineering, Northwestern Polytechnical University, Xi'an 710072, People's Republic China; **G. Zhang, C. Zhang, H. Liao,** and **C. Coddet**, LERMPS, Université de Technologie de Belfort-Montbéliard, Site de Sévenans, Belfort Cedex 90010, France; and **O. Elkedim**, FEMTO ST, UMR CNRS 6174, Université de Technologie de Belfort-Montbéliard, Site de Sévenans, Belfort Cedex 90010, France. Contact e-mail: wenyali_ cn@hotmail.com.

react with Al, such as TiN, is technologically important. TiN is thermally stable up to 3300 K and chemically inert to most of common acids (Ref 8). On the other hand, ball milling of the starting powder mixture could benefit the microstructure and wear resistance of TS MMCs (Ref 9). Therefore, in this paper, the effect of ball milling on the microstructure and dry sliding wear behavior of CS Al5356/TiN composite was examined.

2. Experimental Procedure

A gas-atomized Al5356 powder (AlMgCrMnTi, 5-63 μm, LERMPS Lab, France) and a commercial TiN powder (10-45 μm, H.C. STARCK, USA) were used as feedstocks. Table 1 shows the typical properties of Al5356 and TiN bulk in literature (Ref 25, 26). A blend of 50 wt.% (32.7 vol.%) TiN was mechanically mixed (MM) and part of the MM blend was ball-milled (BM) using a planetary ball mill (PM400, RETSCH, Germany). The ball milling was performed at 300 rpm for both the revolution and rotation speeds of stainless steel jars for 40 h (totally 80 h with alternate half-hour rotating and half-hour stop). The ball-to-powder charge ratio was about 11:40 (five stainless steel balls of 30 mm diameter and 400 g powder). After BM, the powder was sieved to <63 μm suitable for spraying. The morphologies of the powders are shown in Fig. 1. It is seen from Fig. 1(a) that Al5356 powder presents a spherical morphology and TiN powder presents an angular shape (Fig. 1b) with some particles agglomerated by fine TiN particulates. The BM powder exhibits an irregular shape (Fig. 1c) with fine TiN particulates agglomerated at Al5356 particle surfaces (Figs. 1d, e). The size distributions of these powders were measured by a laser diffraction sizer (MASTERSIZER2000, Malvern Instruments Ltd., UK). They had a similar size distribution with an average particle size of about 30 μm as shown in Fig. 1(f). For comparison, pure Al5356 deposit was also produced. Al disks having a 25.4 mm diameter and 10 mm thickness were used as substrate and sand-blasted prior to spraying.

Table 1 Properties of Al5356 and TiN bulk in literature (Ref 25, 26)

Material	Density, g/cm^3	Hardness
Al5356	2.64	~50 HB
TiN	5.22	21 GPa

A CS system installed in LERMPS lab with a commercial CS gun (CGT GmbH, Germany) was employed. An optimized nozzle designed by LERMPS was adopted, which had an expansion ratio of about 4.9 and a divergent section length of 170 mm. High-pressure air was used as the accelerating gas at a pressure of 2.7 MPa and a temperature of about 510 °C. Argon was used as powder carrier gas with a pressure of about 3 MPa. The standoff distance from the nozzle exit to the substrate surface was 30 mm. The spray gun was mounted on a robot (ABB, Sweden) and moved with a traverse speed of 200 mm/s.

The microstructure of the deposits was examined by optical microscope (OM) (Nikon, Japan), scanning electron microscope (SEM) (JSM5800LV, JEOL, Japan)

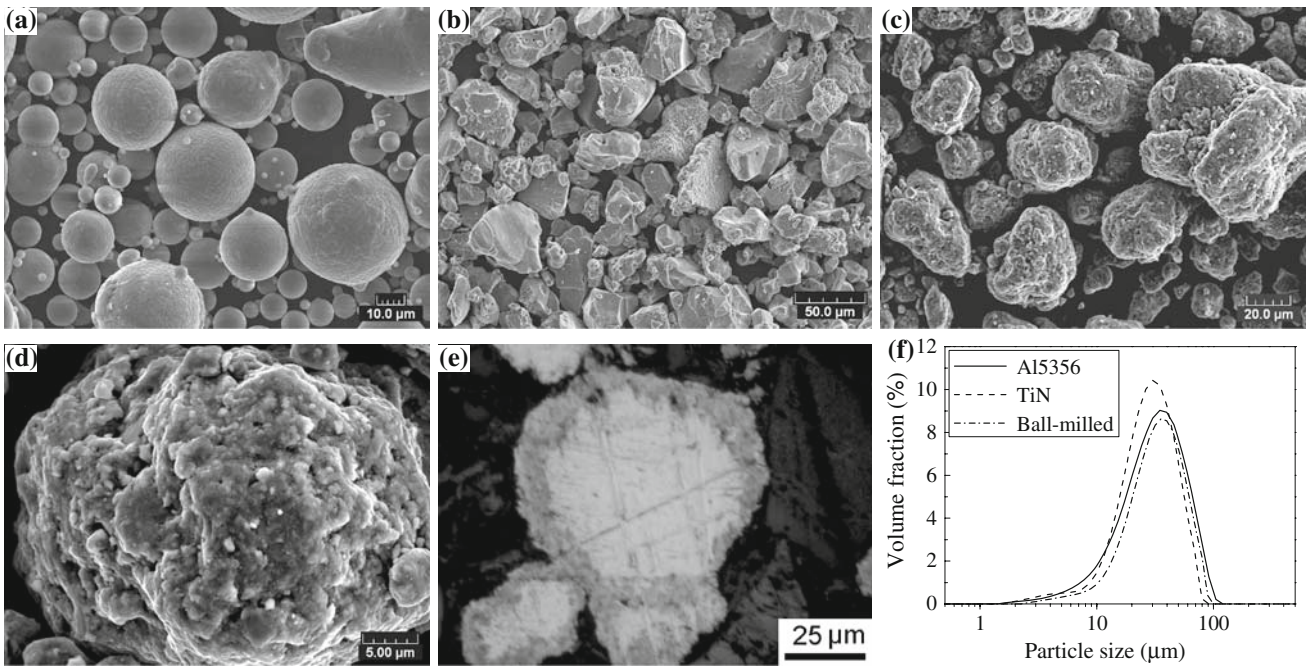

Fig. 1 SEM morphologies of (a) Al5356, (b) TiN and (c, d) BM powders; (e) OM cross section of a BM particle, and (f) size distributions of the used powders

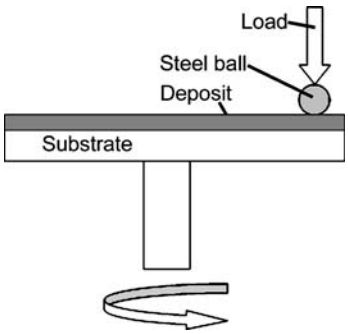

Fig. 2 Schematic diagram of the tribological test apparatus

including energy dispersive X-ray analysis (EDXA), and X-ray diffraction (XRD) (D8 Advance, Brucker AXS, Germany) analysis with Cu $K\alpha_1$ radiation. The porosities and TiN volume fractions of the deposits were estimated from more than 10 cross-sectional OM micrographs through the image analysis with Scion Image (NIH, USA).

The microhardness of the deposits was tested by a Vickers hardness indenter (Leitz, Germany) under a load of 200 g and a dwell time of 15 s. More than 15 values from random locations on the central region of polished cross section were averaged.

The adhesive strengths of coatings were conducted using the ASTM standard C633-01. Coatings of a thickness of about 300 μm were produced. After deposition, the uncoated surface of sample was sand-blasted, and then both the coating and uncoated surfaces were glued to two prepared samples (with internal screw) using an adhesive (FM1000, MOSAVIA Corporation, USA). The assembled parts were then tested in a tensile testing machine (ESCOTEST 50, Germany) after cured at 185 °C for 2 h. Three samples were used for each group.

Friction tests were performed on a ball-on-disc CSM tribometer under an ambient environment (temperature: 19 °C, humidity: 58%). The schematic diagram of the tribological test apparatus is illustrated in Fig. 2. Before friction tests, all deposit surfaces were polished to a roughness (R_a) of about 0.15 μm. The counterpart is a 6 mm diameter 100Cr6 steel ball with a mirror-finished surface. The applied load and sliding velocity were 2 N and 0.2 m/s, respectively. The sliding diameter and distance were 14 mm and 50 m, respectively. The mean coefficient of friction (COF) was estimated from the data between the sliding distances of 5-50 m as shown in Fig. 6. The wear rate (WR) is defined as the worn volume per unit of the applied load and sliding distance. The cross-sectional areas of worn tracks were obtained using an Altisurf500 profilometer. 8 cross-sectional areas obtained for different positions of a worn track were averaged. The total worn volume can be obtained by multiplying the cross-sectional area of worn track and its perimeter. However, owing to the poor wear resistance of pure Al5356 deposit, the friction test was redone for Al5356 deposit in a sliding distance of 1 m for a better investigation of worn surfaces.

3. Results and Discussion

3.1 Coating Microstructure

The detailed results on the pure Al5356 deposit and Al5356/TiN composites deposited with the MM blend (MM composite) have been given in the previous paper (Ref 27). Fig. 3 shows the cross-sectional OM and SEM micrographs of the Al5356/TiN composite deposited with the BM blend (BM composite). It is seen from Fig. 3(a) that BM composite presents a dense structure as observed for MM composite (Ref 27). The porosities of both BM and MM composites were estimated to be less than 1%, which is much less than that of the pure Al5356 coating with an average porosity of 2.9 ± 0.9% (Ref 27). It could be attributed to the low density of Al5356 as shown in Table 1 and thus a decreasing kinetic energy (Ref 12, 14, 17). The larger density of TiN than Al5356 enhances the kinetic impacting process and thus a denser deposit during the co-deposition process. On the other hand, the coating presents a well bond with the Al substrate as shown in Fig. 3(a). The XRD results shown in Fig. 4 indicate that the coating presents the same phase structure as the original powder and almost no oxidation occurs during CS, which is consistent with the other cold sprayed metallic coatings.

In addition, TiN particles are uniformly dispersed in the BM composite, which can be clearly seen from Figs. 3(b) and (c). The distribution of TiN particles is more uniform than those in the MM composites as reported in the previous study (Ref 27). More fine TiN particulates present in the BM composite (See Fig. 3(c)). The TiN volume fraction in the composite deposited with the MM composite was 31.4 ± 5.2 vol.%. However, it is difficult to estimate the TiN volume fraction in the BM composite owing to the dispersed superfine TiN particulates. Through the estimation of several micrographs, the TiN volume fraction in the BM composite was about 53.2 ± 10.8 vol.% with a large statistical error. However, this value is consistent with the results obtained for the MM composite (60.8 ± 7.7 vol.%, 75 wt.% TiN in feedstock, Ref 27), which has the similar microhardness with this BM composite. The previous study (Ref 27) showed that the TiN volume fraction in the composite increased with the increase of TiN volume fraction in the feedstock. Through a detailed observation of the BM powder, it could be considered that the ball milling process leads to a relatively high TiN volume fraction compared with the corresponding blend. Therefore, a higher TiN volume fraction was obtained in the BM composite.

3.2 Coating properties

As shown in Table 2, the microhardness of the MM and BM composites was significantly increased compared to that of Al5356 deposit. It is clear that the composite has been reinforced by the uniformly distributed TiN particles. For the BM composite, the microhardness was further increased. This could be attributed to the refinement of TiN particles and the increase of TiN volume fraction in

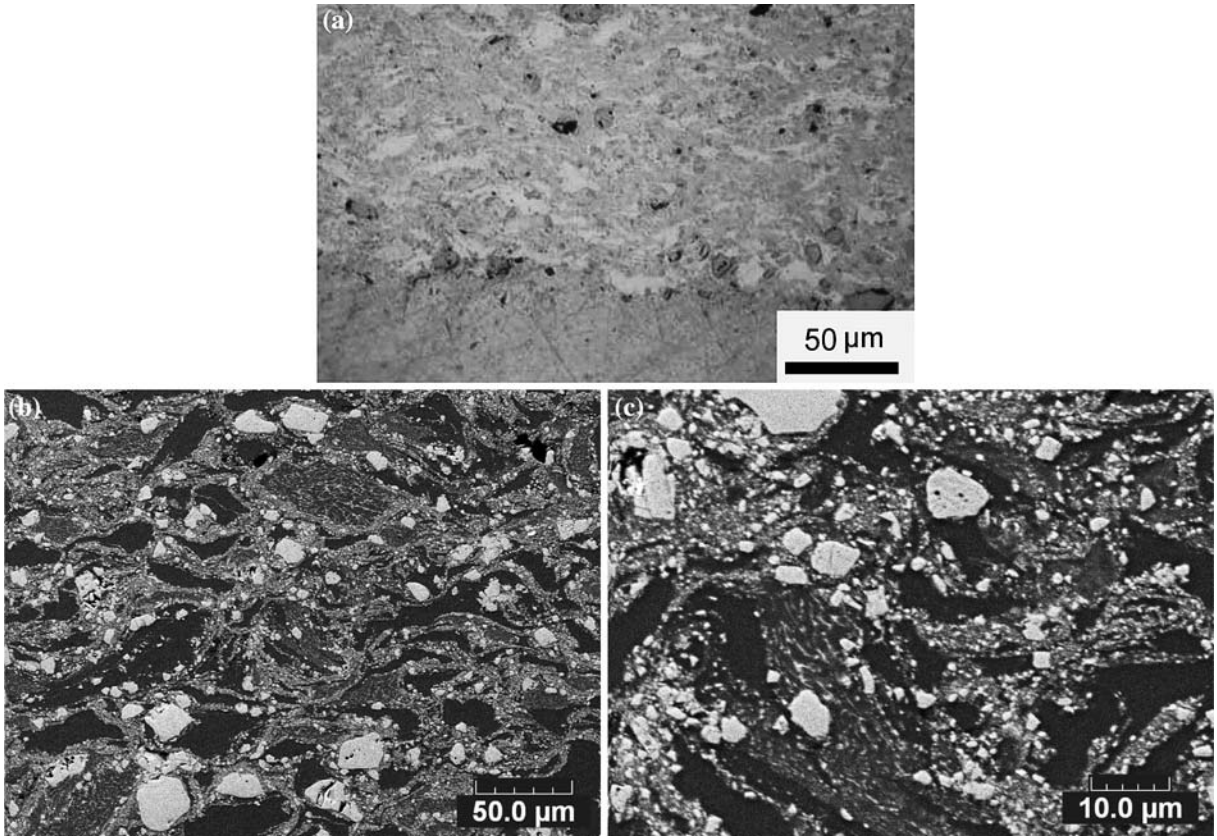

Fig. 3 Typical OM (a) and SEM (backscattered electrons) micrographs (b, c) of cross section of BM composite. (b) High magnification of (c). Bright phase is TiN and dark phase is Al5356 in (b, c)

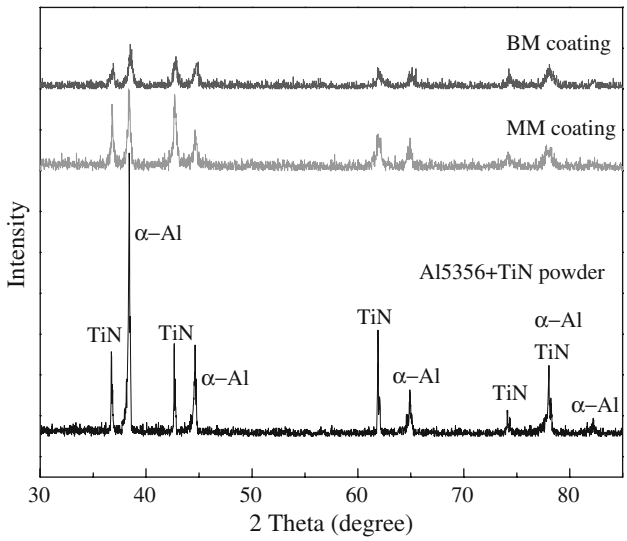

Fig. 4 XRD results of the feedstock blend and the deposited MM and BM coatings

the BM composite as discussed above. Moreover, these values are comparable to those of AMMs produced by powder metallurgy (Ref 3, 5) and CS with different spray conditions (Ref 18, 19) although different reinforcements were used. The strain-hardening effect during deposition can contribute to the increasing hardness of Al5356 deposit. While for the composites, it is clear that besides the strain-hardening effect, the uniformly dispersed TiN particles strengthen the matrix by restricting the matrix deformation.

The adhesive strength of the coatings is also given in Table 2. The adhesive strength of pure Al5356 deposit was about 32 MPa. The failure occurs at deposit/substrate interface with some particles remained at substrate surface. While for the composite deposits, the adhesive strength was much improved to higher than 50 MPa. All the samples fractured in the adhesive during the tensile test. The pinning effect effectuated by TiN particles on the deposited Al5356 particles is responsible for this increase. Fig. 5 shows the cross-sectional fracture morphologies of BM composite obtained from bending the substrate to peel the coating. Similar to the MM composites (Ref 27), the BM composite present a distinguishing fracture pattern from the pure Al5356 deposit, where the fracture mostly occurred at the week interfaces between the deposited particles. It seems that the fracture occurred from both the interfaces between TiN particles with the matrix and those between the deposited Al5356 particles. Apparently, the deposited Al5356 particles in the composite presented higher plastic deformation before the fracture occurred. This fact is closely related to the

Table 2 Experimental results on deposit microhardness, friction coefficient, and wear rate

Deposit	Microhardness ($Hv_{0.2}$)	Adhesive strength, MPa	Friction coefficient	Wear rate, $\times 10^{-4}$ $mm^3/(m\ N)$
Al5356	68.7 ± 11.6	32 ± 4	0.75 ± 0.08	36.1 ± 1.4
MM blend	183.5 ± 13.0	>50 (a)	0.42 ± 0.02	2.5 ± 0.5
BM blend	250.5 ± 38.8	>50 (a)	0.38 ± 0.03	0.7 ± 0.3

(a) Note that the failure occurs in the used adhesives

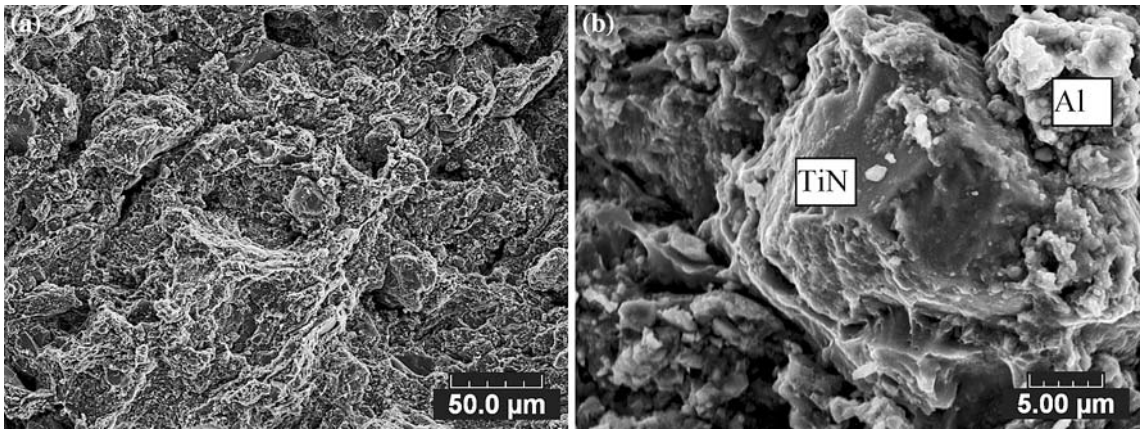

Fig. 5 Fractographs of BM composite obtained by bending the substrate to peel the coating, (b) high magnification of (a)

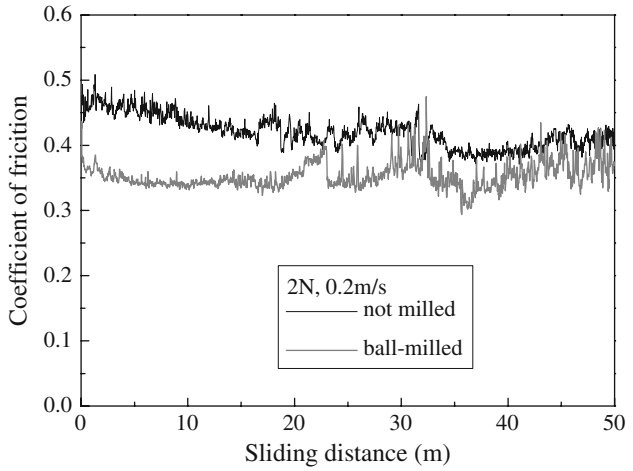

Fig. 6 Evolution of friction coefficients of MM and BM composites versus sliding distance

pinning effect of the ceramic particles on the deposited Al5356 particles.

Fig. 6 shows the typical evolution of the friction coefficients of MM and BM composites versus the sliding distance. After a very short run-in period, the friction coefficient arrives at a relatively steady state. It is seen that the BM composite present a little lower friction coefficient than the MM composite. The mean friction coefficients of the deposits estimated from the data between the sliding distances of 5-50 m are presented in Table 2. The standard deviation represents the variation of COF during sliding. As expected and indicated in Table 2, both the MM and BM composites present a lower COF than pure Al5356 deposit. The BM composite had a slightly lower COF than the MM composite. Furthermore, the WRs of the MM and BM composites were respectively decreased by about 14 and 50 times compared to that of Al5356 deposit. That means the WR of the BM composite was more than 3 times lower than that of the MM composite. On the other hand, the WR of BM composite was just half of that of the MM composite deposited with the 75 wt.% TiN feedstock, which has the similar TiN volume fraction, microhardness and COF with the BM composite as reported in Ref 27. These results are also comparable to those of Al-TiN composites fabricated through a powder metallurgical route (Ref 8).

As discussed in paper (Ref 27), the adhesion between the deposit and the sliding ball is a dominant factor for the tribological behavior of pure Al5356 deposit, which present as the typical brim-like shapes in the worn surface. These brim-like shapes were assumed to be formed by the superior deformation of the surface materials along the sliding direction over that of the sub-surface (Ref 28). For the composites, almost no brim-like shape was found on the worn surfaces (Ref 27). On the contrary, many fine TiN particulates distributed on the worn surfaces. This indicated that adhesion was no longer a dominant factor for the composites. Under a shearing force, the surface layer involved in the frictional process, exhibited a decreased parallel deformation due to the pinning effect of TiN particles. In addition, these fine particles could contribute to a third-body abrasion in the following sliding process, which benefits the decrease of friction by means

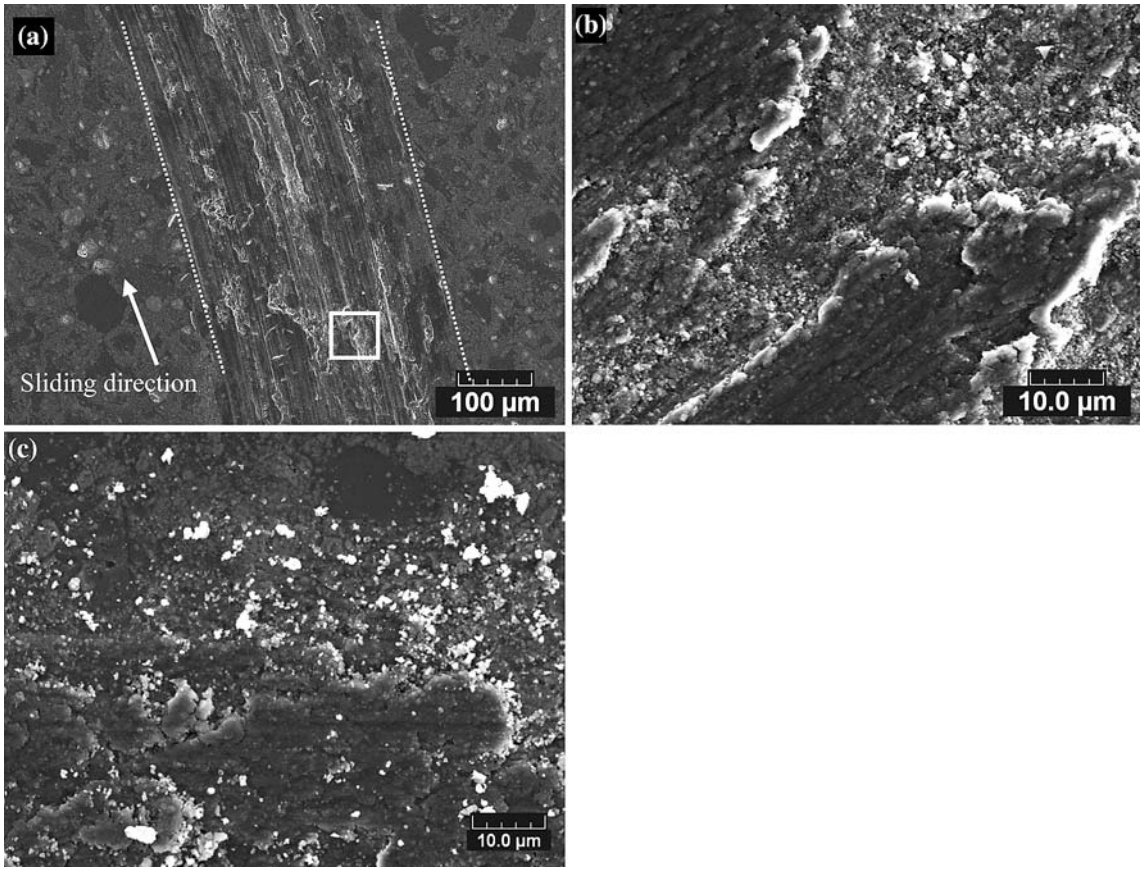

Fig. 7 Worn surfaces of the BM composite

of rolling action partially instead of sliding action. Fig. 7 shows the morphologies of worn track of the BM composite. It was found that the width of worn trance was less than that of the MM composite (Ref 27). For the BM composite, more and finer TiN particles were found in the worn trace as shown in Figs. 7(b) and (c), which appears more like that of the MM composite deposited with the 75 wt.% TiN feedstock (Ref 27). Therefore, taking into account the third-body rolling action, it could be considered that the superfine TiN particulates are attributed to the further decreasing of COF and WR of BM composite in this study.

4. Conclusions

The results clearly show that CS is a promising process to fabricate the AMMCs. With the help of ball milling of the feedstock, the deposited composite coating presents an excellent performance compared to that of the composite sprayed without using the BM powder. The dense Al5356/TiN composites with TiN particles uniformly dispersed in the matrix and a porosity of less than 1% were produced by CS using both the MM and BM blends. The microhardness of the composites was much higher than that of pure Al5356 deposit and increased significantly through ball-milling of the feedstock. The adhesive strength of the composites was remarkably improved owing to the pinning effect of TiN particles. The COF and WR of the composites were much lower than those of pure Al5356 coating. The COFs of the composites was almost half of that of pure Al5356 coating, while the WRs of the MM and BM composites were, respectively, decreased by about 14 and 50 times than that of pure Al5356 deposit. This fact could be attributed to the third-body abrasion effect by the fine TiN particulates present in the worn surface in the following sliding process, which benefits the decrease of COF by rolling action instead of sliding action. For the BM composite, more and finer TiN particles present in the worn surface compared to the MM composite, which will be helpful to the further decrease of the COF and WR.

Acknowledgments

This work was financially supported by Franche-Comte Regional Council of France. The authors would like to thank Lucas Dembinski of LERMPS for the supply of Al5356 powder.

References

1. C.T. Yu, J.Z. Cui, and L. Wang, Metal Matrix Composites. Metallurgical Industry Press, Beijing, 1995, in Chinese
2. A.M. Davidson and D. Regener, A Comparison of Aluminium-based Metal-matrix Composites Reinforced with Coated and Uncoated Particulate Silicon Carbide, *Compos. Sci. Technol.*, 2000, **60**(6), p 865-869
3. D.P. Mondal and S. Das, High Stress Abrasive Wear Behaviour of Aluminium Hard Particle Composites: Effect of Experimental Parameters, Particle Size and Volume Fraction, *Tribol. Int.*, 2006, **39**(6), p 470-478
4. Y. Yalcin and H. Akbulut, Dry Wear Properties of A356-SiC Particle Reinforced MMCs Produced by Two Melting Routes, *Mater. Design*, 2006, **27**(10), p 872-881
5. Y.L. Shen, J.J. Williams, G. Piotrowski, N. Chawla, and Y.L. Guo, Correlation Between Tensile and Indentation Behavior of Particle-reinforced Metal Matrix Composites: an Experimental and Numerical Study, *Acta Mater.*, 2001, **49**(16), p 3219-3229
6. A. Slipenyuk, V. Kuprin, Y. Milman, V. Goncharuk, and J. Eckert, Properties of P/M Processed Particle Reinforced Metal Matrix Composites Specified by Reinforcement Concentration and Matrix-to-Reinforcement Particle Size Ratio, *Acta Mater.*, 2006, **54**(1), p 157-166
7. J.N. Hall, J.W. Jones, and A.K. Sachdev, Particle Size, Volume Fraction and Matrix Strength Effects on Fatigue Behavior and Particle Fracture in 2124 Aluminum-SiCp Composites, *Mater. Sci. Eng. A*, 1994, **183**(1-2), p 69-80
8. A.K. Ray, K. Venkateswarlu, S.K. Chaudhury, S.K. Das, B.R. Kumar, and L.C. Pathak, Fabrication of TiN Reinforced Aluminium Metal Matrix Composites Through a Powder Metallurgical Route, *Mater. Sci. Eng. A*, 2002, **338**(102), p 160-165
9. Fr.-W. Bach, L. Engl, and L.A. Josefiak, Development of Light Metal Matrix Composite Coatings Using High Velocity Thermal Spray Processes, *Thermal Spray 2003: Advancing the Science and Applying the Technology*, C. Moreau and B. Marple, Eds., May 5-8, 2003 (Orlando, FL, USA), ASM International, OH, 2003, p 769-777
10. A. Papyrin, Cold Spray Technology, Advanced Materials & Processes, *Adv. Mater. Process.*, 2001, **159**(9), p 49-51
11. T. Stoltenhoff, H. Kreye, and H.J. Richter, An Analysis of the Cold Spray Process and Its Coating, *J. Therm. Spray Technol.*, 2002, **11**(4), p 542-550
12. W.-Y. Li, C. Zhang, H.T. Wang, and C.-J. Li, Significant Influences of Metal Reactivity and Oxide Films at Particle Surfaces on Coating Microstructure in Cold Spraying, *Appl. Surf. Sci.*, 2007, **253**(7), p 3557-3562
13. W.-Y. Li, X.P. Guo, C. Verdy, L. Dembinski, H.L. Liao, and C. Coddet, Improvement of Microstructure and Property of Cold-sprayed Cu-4 at.% Cr-2 at.% Nb Alloy by Heat Treatment, *Scripta Mater.*, 2006, **55**(4), p 327-330
14. D.T. Morelli, A.A. Elmoursi, T.H. Van Steenkiste, D.W. Gorkiewicz, and B. Gillispie, Kinetic Spray of Aluminum Metal Matrix Composites for Thermal Management Applications, *Thermal Spray 2003: Advancing the Science and Applying the Technology*, B.R. Marple and C. Moreau, Eds., ASM International, OH, 2003, p 85-90
15. G.L. Eesley and A.N. Elmoursi Patel, Thermal Properties of Kinetic Spray Al-SiC Metal Matrix Composite, *J. Mater. Res.*, 2003, **18**(4), p 855-860
16. F. Gärtner, T. Stoltenhoff, T. Schmidt, and H. Kreye, The Cold Spray Process and Its Potential for Industrial Applications, *Thermal Spray Connects: Explore Its Surfacing Potential*, E. Lugscheider, Ed., DVS, Düsseldorf, 2005 (in CD-ROM)
17. T.H. Van Steenkiste, A. Elmoursi, D. Gorkiewicz, and B. Gillispie, Fracture Study of Aluminum Composite Coatings Produced by the Kinetic Spray Method, *Surf. Coat. Technol.*, 2005, **194**(1), p 103-110
18. H. Weinert, E. Maeva and V. Leshchynsky, Low Pressure Gas Dynamic Spray Forming Near-net Shape Parts, *Thermal Spray 2006: Building on 100 Years of Success*, B.R. Marple, M.M. Hyland, Y.C. Lau, R.S. Lima, and J. Voyer, Eds., May 15-18, 2006 (Seattle, WA), ASM International, Materials Park, OH, 2006
19. J. Haynes, A. Pandey, J. Karthikeyan, and A. Kay, Cold Sprayed Discontinuously Reinforced Aluminum, *Thermal Spray 2006: Building on 100 Years of Success*, B.R. Marple, M.M. Hyland, Y.C. Lau, R.S. Lima, and J. Voyer, Eds., May 15-18, 2006 (Seattle, WA), ASM International, Materials Park, OH, 2006
20. H.K. Kang and S.B. Kang, Tungsten/Copper Composite Deposits Produced by a Cold Spray, *Scripta Mater.*, 2003, **49**(12), p 1169-1174
21. T. Novoselova, P. Fox, R. Morgan, and W. O'Neill, Experimental Study of Titanium/aluminium Deposits Produced by Cold Gas Dynamic Spray, *Surf. Coat. Technol.*, 2006, **200**(8), p 2775-2783
22. S. Marx, A. Paul, A. Köhler, and G. Hüttl, Cold Spraying—Innovative Layers for New Applications, *Thermal Spray connects: Explore Its Surfacing Potential*, E. Lugscheider, Ed., May 2-4, 2005 (Basel, Switzerland), DVS, 2005, p 209-215
23. L. Ajdelsztajn, B. Jodoin, G.E. Kim, and J.M. Schoenung, Cold Spray Deposition of Nanocrystaline Aluminum Alloys, *Metall. Mater. Trans. A*, 2005, **36**(3), p 657-666
24. H.J. Kim, C.H. Lee, and S.Y. Hwang, Superhard Nano WC-12%Co Coating by Cold Spray Deposition, *Mater. Sci. Eng. A*, 2005, **391**(1-2), p 243-248
25. MatWeb, http://www.matweb.com. Accessed 10 April 2007
26. R.S. Guo, S. Cai, H.M. Ji, and H.Z. Wu, Engineering Structural Ceramics. Tianjing University Press, Tianjin, China, 2002, in Chinese
27. W.-Y. Li, G. Zhang, X.P. Guo, H.L. Liao, and C. Coddet, Characterizations of Cold-sprayed TiN Particle-Reinforced Al Alloy-Based Composites—From Structures to Tribological Behaviour, *Adv. Eng. Mater.*, 2007, **9**, p 577-583
28. J. Liu, Material Wear Principle and Wear Resistance. Tsinghua University Press, Beijing, 1993, in Chinese